doi:10.3788/gzxb20184702.0212002

数字散斑干涉术和时空三维相位解包裹用于非连续表面动态变形测量

吴思进[1],杨靖[1],潘思阳[2],李伟仙[1],杨连祥[3]

(1 北京信息科技大学 仪器科学与光电工程学院,北京 100192)

(2 大唐移动通信设备有限公司,北京 100083)

(3 奥克兰大学 机械工程系,美国 罗彻斯特 48309)

摘 要:为解决传统相位解包裹法不能够用于非连续表面的动态变形测量的缺点,在详细阐述基于时空三维相位解包裹技术的数字散斑干涉术的工作原理和测量步骤基础上,应用数字散斑干涉术和时空三维相位解包裹测量非连续表面动态变形.实验证明,当采用每秒 70 帧的普通相机拍照时,可实现最快形变速率为 25.12 μm/s 的非连续表面动态变形测量.本文所提方法扩展了数字散斑干涉术的测量范围,增强其应用能力.

关键词:电子散斑干涉术;变形测量;动态测量;相位分布;振动测量;相位解包裹;非连续表面

中图分类号:O439 **文献标识码**:A **文章编号**:1004-4213(2018)02-0212002-9

Dynamic Deformation Measurement of Discontinuous Surfaces Using Digital Speckle Pattern Interferometry and Spatiotemporal Three-dimensional Phase Unwrapping

WU Si-jin[1], YANG Jing[1], PAN Si-yang[2], LI Wei-xian[1], YANG Lian-xiang[3]

(1 *School of Instrumentation Science and Opto-electronics Engineering, Beijing Information Science and Technology University, Beijing* 100192, *China*)

(2 *Datang Mobile Communications Equipment Co., Ltd, Beijing* 100083, *China*)

(3 *Department of Mechanical Engineering, Oakland University, Rochester, Michigan* 48309, *USA*)

Abstract: Digital Speckle Pattern Interferometry (DSPI) with a Spatiotemporal Three-dimensional Phase Unwrapping (STPU) is used to measure the dynamic deformation distributions with the presence of object discontinuities. It overcomes the phase unwrapping failure of traditional DSPI in such conditions. Elaborate description of the measurement priciple and procedure of the DSPI with STPU is given. The experiments exibited that dynamic deformation of discontinuous surface, with a maximum deformation rate of 25.12 μm/s, can be determined perfectly by the proposed method while an ordinary camera with 70 fps was used. The research benefits the enlargement of the application areas of DSPI and the improvement of its applicability.

Key words: Electronic Speckle Pattern Interferometry (ESPI); Deformation measurements; Dynamic measurements; Phase distribution; Vibration measurement; Phase unwrapping; Discontinuous surface

OCIS Codes: 120.6160; 100.5088; 100.3175; 120.2880; 120.7280

Foundation item: The National Natural Science Foundation of China (Nos. 51675055, 11672045) and the National Major Scientific Instrument and Equipment Development Project of China (No.2016YFF0101801)

First author: WU Si-jin (1979—), male, associate professor, Ph.D. mainly focuses on digital speckle pattern interferometry and digital shearography. Email:swu@bistu.edu.cn

Received: Jul.25, 2017; **Accepted**: Oct.23, 2017

0 Introduction

Digital Speckle Pattern Interferometry (DSPI), also known as Electronic Speckle Pattern Interferometry (ESPI), is a full-field, non-contact, high-accuracy optical measurement technique for micro/nano-deformation measurement, which has been widely used in manufacturing, aerospace, biomedicine, and so on[1-3]. Precise measurement of deformation by DSPI depends on quantitative determination of interferometric phase. The obtained raw phase is wrapped and varies within the range of $[0, 2\pi)$ because of the use of an inverse tangent calculation, an essential process in phase determination[4-5]. This wrapped form causes phase discontinuities which should be removed before the calculation of deformation. The process of phase discontinuity removal is called as phase unwrapping.

Traditionally, Spatial Phase Unwrapping (SPU) is the dominant phase unwrapping algorithm that is used in DSPI. It demodulates phase along a two-dimensional spatial path which is either a predetermined or varying path. Distinguished by strategies of routing, a variety of SPUs have been proposed, including row-by-point algorithm[6], quality-guided algorithm[7], least-squares algorithm[8], branch-cut algorithm[9], minimum L^p-norm algorithm[10], etc. These SPUs can generate high-quality unwrapped phase maps in most cases, due to the use of modern image sensor with millions of pixels. The high-density image sensor allows an over sampling of the wrapped phase map, avoiding fault in phase unwrapping. However, in the presence of object surface discontinuity, abrupt phase change appears, causing local ultrahigh frequency phase variation which is over the image sensor sampling frequency. The local ultrahigh frequency blocks the path of phase unwrapping, resulting in the failure of real phase distribution obtainment. The dependence on continuous phase unwrapping path leads to the failure of using DSPI with SPU to determine phases of discontinuous surfaces.

An alternate to solve the problem is the utilization of Temporal Phase Unwrapping (TPU) in DSPI. TPU demodulates the phase through the time axis, so it can neglect the spatial relation between areas of the object surface[11]. Object discontinuity is not a handicap any longer when phase unwrapping. Another advantage is the determination of absolute phase value which is realized by recording the initial phase map before loading[12]. The disadvantage of TPU is high demand of camera speed which defines the sampling rate of TPU. Unfortunately, the sampling rate cannot satisfy the sampling theory in most situations, even if high-speed cameras are used. This makes DSPI with TPU an unpractical tool in engineering.

Recently, we have proposed a Spatiotemporal Three-dimensional Phase Unwrapping (STPU) which demodulates the phase not only along the two-dimensional spatial path but also through the time axis[13]. The combination of phase unwrapping in spatial and temporal domains makes DSPI able to determine the absolute phase by using an ordinary camera. The ability of the new algorithm in deformation measurement of discontinuous surfaces is also briefly introduced but has not been demonstrated clearly yet. In this article, the principle and procedure of using DSPI with STPU to measure deformation of discontinuous surface are demonstrated in detail. The capability of STPU is further revealed by theoretical explanation as well as experiments.

1 Principle of spatiotemporal three-dimensional phase unwrapping

The original phases obtained by DSPI are wrapped as modulo 2π of the true phases. The relation between the original and true phases is mathematically formulated as

$$\phi = \mathrm{mod}\,(\Phi, 2\pi) = \Phi + 2n\pi \tag{1}$$

where $\phi \in [0, 2\pi)$ is the original phase, Φ is the true phase, and n is an integer.

The process of changing the original phase to the real phase is called as phase unwrapping which is traditionally classified as SPU and TPU, depending on phase unwrapping in spatial or temporal domain respectively.

1.1 Spatial phase unwrapping

SPU compares the phase values at neighboring pixels and adds or subtracts 2π if the phase jumps exist. The unwrapping path is predetermined or varied. Distinguished by strategies of routing, many SPUs have been proposed. For simplicity, row-by-point algorithm, the simplest SPU, is chosen to explain the

basic principle of SPU. Row-by-point algorithm takes the first pixel, usually locating at the lower left corner of the phase map, as a start point. Then from this point, it demodulates the phase along the first column. The phase values at the first column are expressed by

$$\Phi(i,0)=\phi(0,0)+\sum_{i=1}^{m-1}W[\Delta\phi(i,0)] \tag{2}$$

where $\phi(0,0)$ is the phase at the start point, $\Delta\phi$ is the difference between two neighboring pixels along the column, W denotes the operation of elimination of phase jump, m is the height of phase map. Taking the corresponding phase values at the first column as secondary start points, the real phases at the whole phase map are demodulated along each row by using the same method.

Row-by-point algorithm is simple and fast, but will most likely result in phenomena of wire drawing and order jumping when phase unwrapping. These undesirable phenomena will be partly eliminated if other SPUs are used, for example branch-cut algorithm. However, the absolute phase cannot be determined due to the undefined phase value of the start point. Moreover, all SPUs will fail to get correct real phases if complete discontinuities of object surface exist.

1.2 Temporal phase unwrapping

TPU is an idea approach to solve the problems existed in SPU. It is a one-dimensional phase unwrapping algorithm which demodulates phases through the time axis. The first phase map corresponding to the state before loading acts as the zero reference, yielding absolute phase distribution on each phase map. Furthermore, the independence of a pixel from its neighboring pixels let the TPU ignore the surface discontinuities. The algorithm can be expressed by

$$\begin{cases} t=t_0,t_1,t_2,t_3\cdots\cdots s \\ c(t_i)=\mathrm{NINT}\left(\dfrac{\Delta\Phi_{\mathrm{w}}(t_i,t_{i-1})}{2\pi}\right) \\ c(t_0)=0 \\ \Phi_{\mathrm{u}}(t_i)=\Phi_{\mathrm{w}}(t_i)-2\pi\times\sum_{t=t1}^{ti}c(t) \end{cases} \tag{3}$$

where t is time, s denotes the last moment, NINT represents the nearest integer, $\Delta\Phi_{\mathrm{w}}(t_i,t_{i-1})$ represents the phase difference between t_i and t_{i-1}, the subscript w and u denote wrapped and unwrapped respectively. However, to demodulate the whole-field phase maps, TPU is asked to satisfy the sampling theorem at all pixels. It means the frame rate of camera should be high enough so that it can match the highest deformation rate. This is not always satisfied even if high-speed cameras are used. Moreover, the insufficiency of phase information leads to low-quality real phase map which degrades the DSPI's performance.

1.3 Spatiotemporal three-dimensional phase unwrapping

STPU demodulates the phase not only along the two-dimensional spatial path but also through the time axis. This feature makes STPU an idea method to determine real phase of a discontinuous surface. The first step of STPU is region separation which can be performed automatically or manually by localizing the abnormity of the phase spatial distribution. The phase abnormity is usually caused by surface discontinuities. The automatic region separation is realized by evaluation of the local spatial frequencies of the phase map. Independent region is marked if it is surrounded by a close ring in which there is hyperfrequency phase. After the region separation, reference point searching is performed to find the locations of the lowest frequency phase variation in each separated region, by evaluating the temporal frequencies of the phase variation at all pixels. The characteristic of the reference points is on which the displacement rates are lower enough to be sampled easily. It can be explained by

$$\frac{\partial D(x,y,t)}{\partial t}\leqslant\frac{\lambda}{2k}\cdot f_{\mathrm{frame}} \tag{4}$$

where $\partial D/\partial t$ represents displacement rate, (x,y) denotes the location of reference point, λ is the laser wavelength, k is an integer larger than or equal to 2, and f_{frame} is the frame rate of the camera used in DSPI.

Once the reference points are defined, TPU is utilized to demodulate the phase at each reference point

through the time axis and determine the absolute phase at each step. Taking these reference points as the start points for eachregion, SPU demodulates the phase spatial distribution on each region and obtains the absolute real phase distributions, aided by the definitive phases at the reference points. The whole field real phase maps at different moments are consequently established by combining the phase distributions of each separated region together. The procedure of STPU is shown in Fig.1.

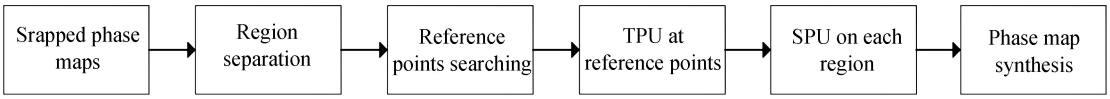

Fig.1 Flowchart of STPU operation

Different from TPU, STPU demodulates the phases through the time axis at several referent points rather than in whole field. The much lower displacement rates of these selected points than those of the whole field, aid in the enhancement of DSPI ability in measurement of high-speed deformations. In most cases, these reference points are not hard to be found because the displacement rates in whole field are always nonuniform and vary noticeably. Consequently, DSPI with STPU is more suitable to practical applications than DSPI with TPU. In comparison with SPU, STPU is able to determine the absolute phases, and furthermore, the phases of discontinuous surfaces. Considering that it can also measure dynamic deformations, DSPI with STPU is a competitive candidate in dynamic deformation measurement of discontinuous surfaces. This conclusion will be verified by the following experiments.

2 Experiments

2.1 Dynamic measurement of cantilever vibration

An optical setup of spatial-carrier DSPI[14], shown in Fig.2, was built to carry out the experiments. The laser beam from a single-longitude semiconductor pumped solid state laser with 532 nm wavelength was divided into object and reference beams. The object beam struck the object, a metal cantilever, after it was expanded. The scattered light was collected by a lens and aperture, and then entered into a camera with 70 fps frame rate @ 2 megapixels, in which it interfered with the reference beam, forming a speckle interferogram as shown in Fig. 3. The speckle interferogram was separated by a shadow which was generated by a stick placed in front of the object. The shadow generated the phase discontinuity, shown in

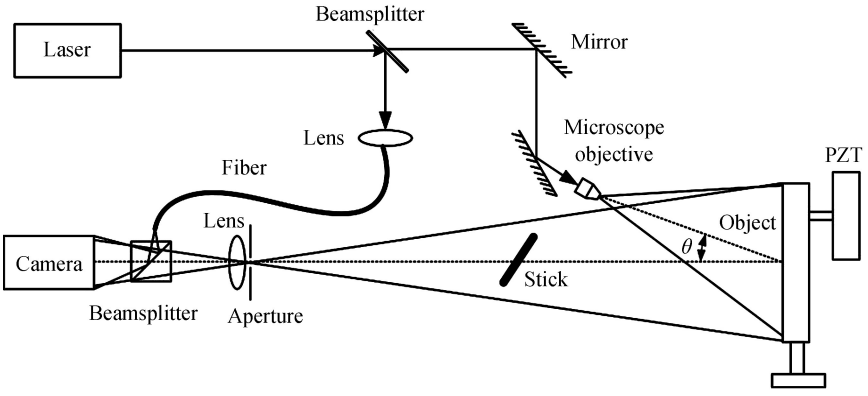

Fig.2 Optical setup of spatial-carrier DSPI

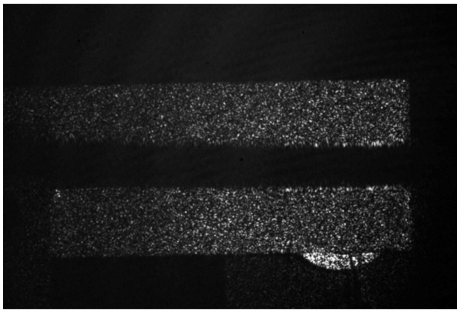

Fig.3 Speckle interferogram

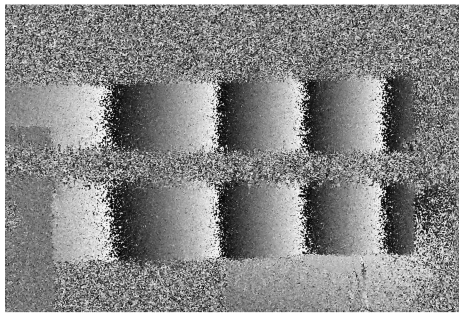

Fig.4 Original phase map

Fig.4, which is similar to those generated by object surface discontinuity. During the measurement, the cantilever beam is excited by a Piezoelectric Transducer (PZT) in the right end with the left end fixed on the base, yielding a sine vibration with a frequency of 4 Hz and a nominal amplitude of 1 μm which cause a phase change of 23.6 rad. The vibration of cantilever was measured by the DSPI, yielding a series of wrapped phase maps. Parts of the obtained phase maps are shown in Fig.5 after they are smoothed.

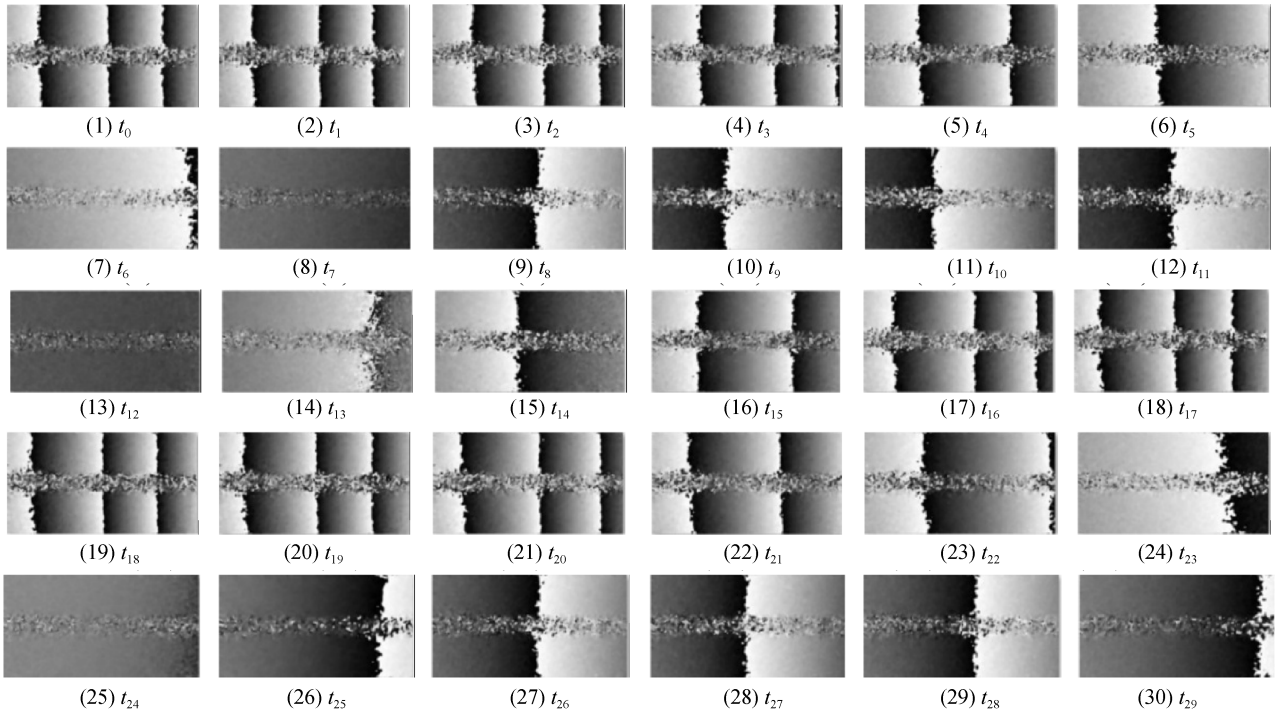

Fig.5 Phase maps of cantilever vibration

In each phase map, the phase distribution is separated into two regions by a belt zone on which the phase with much high-frequency noise appears. This noise zone is formed by the stick shadow which destroys the optical interference. For these phase maps, SPU is unable to generate proper real phase maps due to the totally separated phase regions. TPU can demodulate the phases on the left part in which the displacement rate is low, but fails to get an exact real phase distribution in the right part because of the high displacement rate.

In this experiment, STPU was used to unwrap the phases. It firstly separated the phase map into two regions by distinguishing the border of the noise zone. Two reference points A and B were subsequently localized on the left part of the cantilever. These reference points are chosen by following the criterion described by Eq. (4). Considering it is a sine vibration, the displacement rate can be theoretically expressed by

$$\frac{\partial D(x,y,t)}{\partial t}=2\pi a f\cos\ (2\pi ft+\psi) \tag{5}$$

where a is the amplitude of vibration, f is the frequency of vibration, ψ is the initial phase angle. Considering that the maximum amplitude is, nominally, 1 μm, and vibration frequency is 4 Hz, the maximum displacement rate corresponding to Eq. (5) is 25.12 μm/s. This is beyond the sampling rate of 9.31 μm/s, which is defined by the right part of Eq. (4), so the location where the maximum amplitude appears cannot be chosen as the reference point. Theoretically, locations with amplitude of less than 0.37 μm is suitable for reference points. However, because of the nonperfect sine vibration, the real amplitude could be a little bit bigger than 0.37 μm. In this experiment, the vibration amplitude at points A and B is around 0.42 μm.

Fig.6 shows the phase unwrapping result of reference point A obtained by TPU. The upper part is the original wrapped phase and the lower part depicts the unwrapped phase. It can be found that there are more than 2 sampling points in one 2π phase cycle, guaranteeing the phase can be demodulated correctly by TPU. The reasonable unwrapped phase also verifies the validity of using TPU on this point. The TPU

merely satisfies the phase unwrapping on points A and B's left. It cannot unwrap the phase on their right due to the much higher displacement rate. Consequently, The TPU cannot satisfy the phase unwrapping on the whole field.

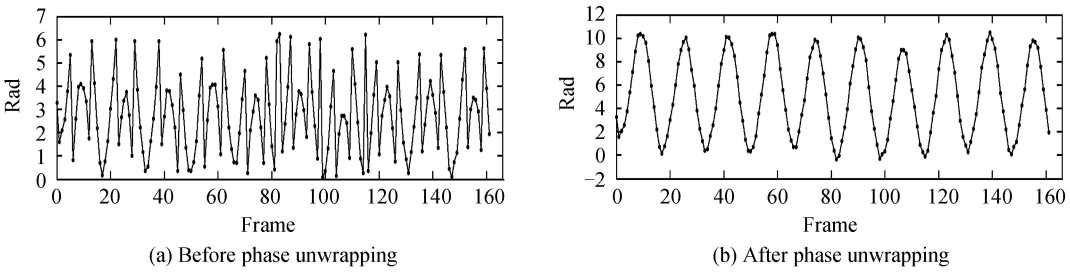

(a) Before phase unwrapping (b) After phase unwrapping

Fig.6 TPU on reference point A

Phase distribution at each moment was given by performing row-by-point SPU on each region after the absolute phases of reference points were determined by TPU. This process is depicted by Fig.7.

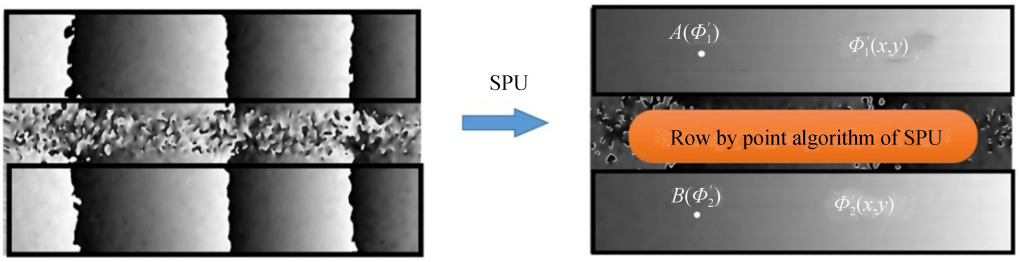

Fig.7 Region separation and SPU

The real phase maps are obtained by combining the two separated absolute phase distributions. The out-of-plane deformation distributions are finally calculated by[15]

$$w=\frac{\lambda}{2\pi(1+\cos\theta)}\Phi \tag{6}$$

where θ represents the object beam illumination angle of the experimental optical setup depicted by Fig.2. Considering the illumination angle is very small, Eq. (6) can be simplified as

$$w=\frac{\lambda}{4\pi}\Phi \tag{7}$$

Fig.8 shows the deformation distribution of the cantilever at one time. The horizontal ordinates indicate the sizes of the object surface while the vertical ordinate denotes the amplitude of the deformation. It demonstrates the dynamic deformation of the cantilever vibration can be exactly measured by the DSPI with a middle-speed camera. Surface discontinuities no longer invalidate the deformation measurement using DSPI when STPU is used.

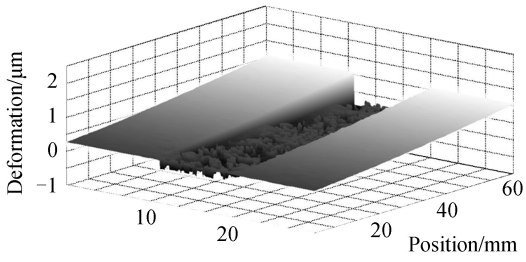

Fig.8 Deformation of the cantilever

If the shadow in the phase map is on a vertical direction, as shown in Fig.9, the absolute deformation can also be obtained by STPU. The results is exhibited in Fig.10. However, in this case, the shadow should be in the left part of the cantilever so that an appropriate reference point can be found in the shadow's right.

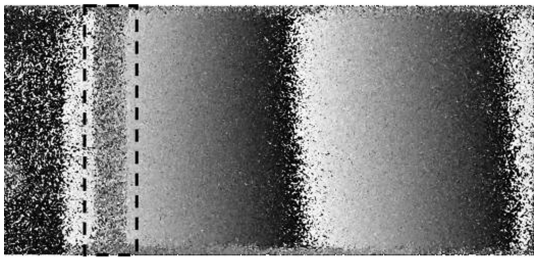

Fig.9 Original phase map with vertical shadow

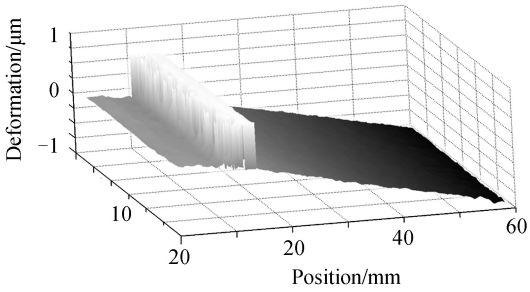

Fig.10 Deformation of the cantilever with discontinuity on vertical direction

2.2 Dynamic measurement of fork vibration

Another example is the dynamic measurement of vibration of fork which surface is discontinuous. The vibration was generated by an electric control PZT with a 4 Hz sinusoid. The same optical setup which is depicted by Fig.2 was used to capture the interferograms. The differences between this experimental setup from the previous setup for cantilever vibration measurement are the camera and the absence of the stick. In this experiment, the surface discontinuity is the attribute of fork, so the stick is not needed. In order to enhance the temporal sampling rate, a camera with 150 fps frame rate @ 1.3 megapixels was used to replace the previous camera. Following the same procedure, the phase maps were obtained in sequence. One of the phase maps is shown in Fig.11 and its corresponding smoothed phase map is shown in Fig.12. The phase map is separated into 4 regions. Four reference points in each separated region were determined by following the criterion given in Eq.(4). The phase map is later unwrapped by the STPU, yielding the absolute phase distribution that is depicted by Fig.13. The deformation distribution is later obtained. Parts of the deformation height maps are showed in Fig.14 to describe the vibration of the fork.

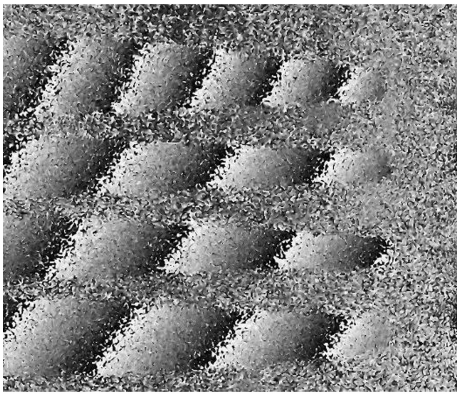

Fig.11 Original phase map of the fork

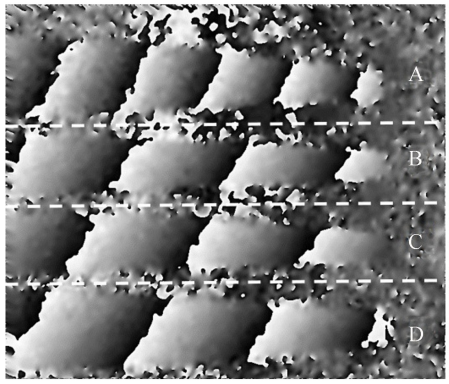

Fig.12 Smoothed phase map of the fork

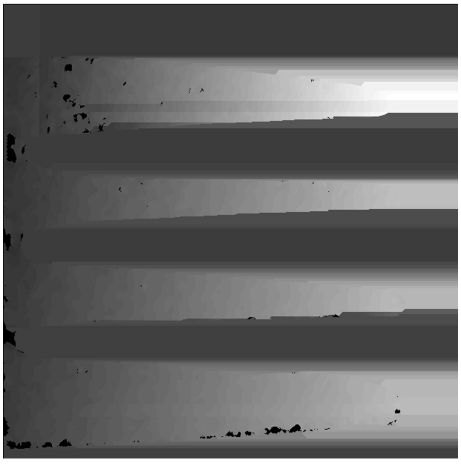

Fig.13 Unwrapped phase map of the fork

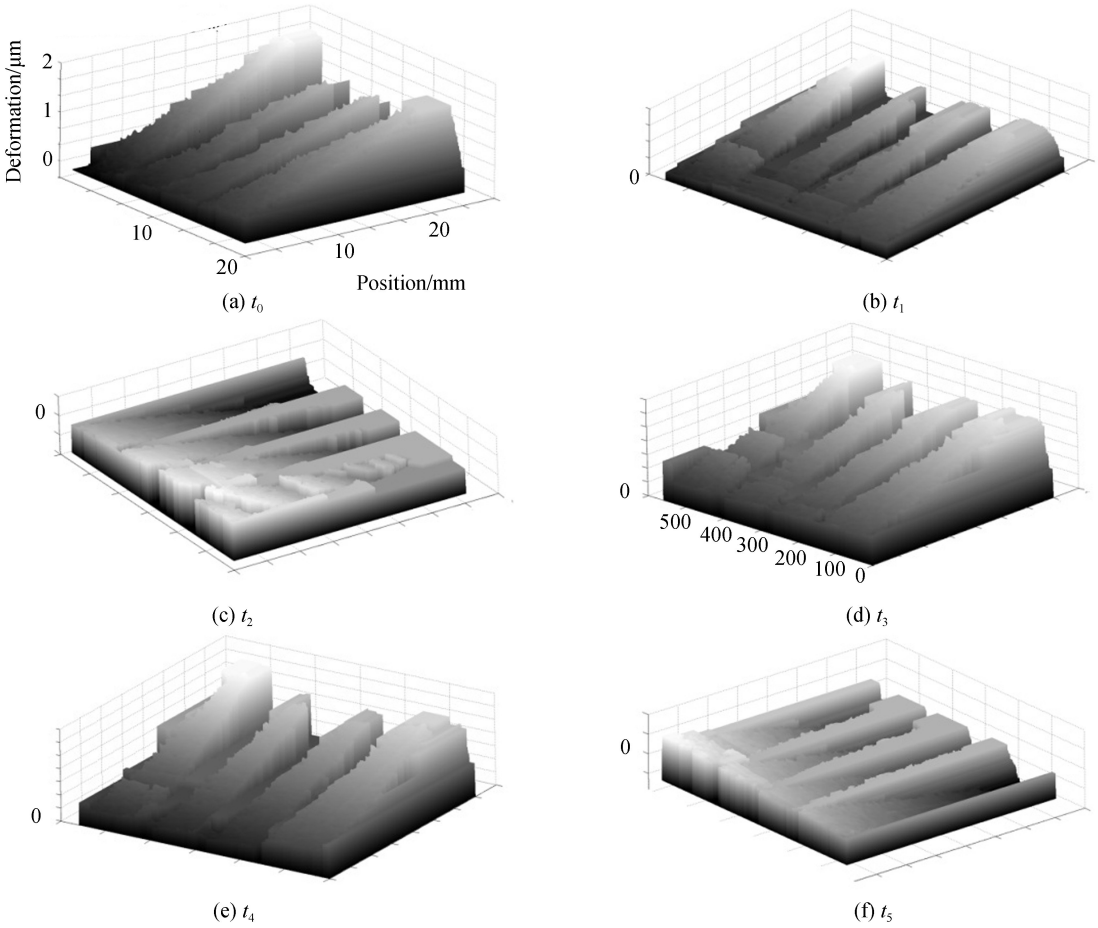

Fig.14 Vibration of fork

3 Conclusion

We demonstrate that dynamic deformation measurement of discontinuous surfaces is carried out by using DSPI and STPU. Its good performance is shown by the experiments. The ability in dynamic measurement of discontinuous surface benefits DSPI in the enlargement of application range and makes DSPI a practical tool in engineering.

References

[1] SUN Ping, HAN Qing, WANG Xiao-feng, *et al*. Technique of 3-D carrier modulation in ESPI and its application in displacement measurement of diesel engine[J]. *Acta Photonica Sinica*, 2007, **36**(7): 1326-1330.

[2] YANG Lian-xiang, XIE Xin, ZHU Lian-qing, *et al*. Review of Electronic Speckle Pattern Interferometry (ESPI) for three dimensional displacement measurement[J]. *Chinese Journal of Mechanical Engineering*, 2014, **27**(1): 1-13.

[3] TIZIANI H J, PEDRINI G. From speckle pattern photography to digital holographic interferometry[J]. *Applied Optics*, 2013, **52**(1): 30-44.

[4] HUANG H Y H, TIAN L, ZHANG Z, *et al*. Path-independent phase unwrapping using phase gradient and total-variation (TV) denoising[J]. *Optics Express*, 2012, **20**(13): 14075-14089.

[5] ZHANG Xiong, QIAN Xiao-fan. An improvement on the least-squares phase unwrapping algorithm for under sampled interferogram[J]. *Acta Photonica Sinica*, 2011, **40**(1): 121-125.

[6] ITOH Kazuyoshi. Analysis of the phase unwrapping algorithm[J]. *Applied Optics*, 1982, **21**(14): 2470.

[7] CHEN Ke, XI Jiang-tao, YU Yan-guang. Quality-guided spatial phase unwrapping algorithm for fast three-dimensional measurement[J]. *Optics Communications*, 2013, **294**(1): 139-147.

[8] DOLINKO A E, KAUFMANN G H. A least-squares method to cancel rigid body displacements in a hole drilling and DSPI system for measuring residual stresses[J]. *Optics and Lasers in Engineering*, 2006, **44**(12): 1336-1347.

[9] SOUZA J C, OLIVEIRA M E, SANTOS P A M. Branch-cut algorithm for optical phase unwrapping[J]. *Optics Letters*, 2015, **40**(15): 3456-3459.

[10] GHIGLIA D C, ROMERO L A. Minimum L^p-norm two-dimensional phase unwrapping[J]. *Journal of the Optical Society of America*, 1996, **13**(10): 1999-2013.

[11] HUNTLEY J M, SALDNER H. Temporal phase unwrapping: application to surface profiling of discontinuous objects [J]. *Applied Optics*, 1997, **36**(13): 2770-2775.

[12] FU Yu, PEDRINI G, OSTEN W. Vibration measurement by temporal Fourier analyses of a digital hologram sequence [J]. *Applied Optics*, 2007, **46**(23): 5719-5727.

[13] WU Si-jin, ZHU Lian-qing, PAN Si-yang, *et al*. Spatiotemporal three-dimensional phase unwrapping in digital speckle pattern interferometry[J]. *Optics Letters*, 2016, **41**(5): 1050-1053.

[14] WU Si-jin, DONG Ming-li, FANG Yao, *et al*. Universal optical setup for phase-shifting and spatial-carrier digital speckle pattern interferometry[J]. *Journal of the European Optical Society-Rapid Publications*, 2016, **12**(1): 14.

[15] JIANG Yan-peng, WU Si-jin, YANG Lian-xiang. Simultaneous measurement of contour and micro-deformation using full-field optical method[J]. *Journal of Applied Optics*, 2017, **38**(1): 67-71.